

## Chemotaxis-induced spatio-temporal heterogeneity in multi-species host-parasitoid systems

Ian G. Pearce · Mark A. J. Chaplain ·  
Pietà G. Schofield · Alexander R. A. Anderson ·  
Stephen F. Hubbard

Received: 6 July 2006 / Revised: 15 February 2007 / Published online: 14 April 2007  
© Springer-Verlag 2007

**Abstract** When searching for hosts, parasitoids are observed to aggregate in response to chemical signalling cues emitted by plants during host feeding. In this paper we model aggregative parasitoid behaviour in a multi-species host-parasitoid community using a system of reaction-diffusion-chemotaxis equations. The stability properties of the steady-states of the model system are studied using linear stability analysis which highlights the possibility of interesting dynamical behaviour when the chemotactic response is above a certain threshold. We observe quasi-chaotic dynamic heterogeneous spatio-temporal patterns, quasi-stationary heterogeneous patterns and a destabilisation of the steady-states of the system. The generation of heterogeneous spatio-temporal patterns and destabilisation of the steady state are due to parasitoid chemotactic response to hosts. The dynamical behaviour of our system has both mathematical and ecological implications and the concepts of chemotaxis-driven instability and coexistence and ecological change are discussed.

**Keywords** Host-parasitoid systems · Reaction-diffusion-chemotaxis models · Chemotaxis driven instability · Spatio-temporal heterogeneity

---

I. G. Pearce gratefully acknowledges the financial support of the NERC.

---

I. G. Pearce (✉) · M. A. J. Chaplain · A. R. A. Anderson  
Division of Mathematics, University of Dundee, Dundee DD1 4HN, UK  
e-mail: ipearce@maths.dundee.ac.uk

P. G. Schofield · S. F. Hubbard  
College of Life Sciences, University of Dundee, Dundee DD1 4HN, UK

## 1 Introduction

In this paper we consider a mathematical model that focuses on the aggregative response of parasitoids to hosts in a coupled multi-species system. Our system comprises two parasitoid species and two host species. The parasitoids are, *Cotesia glomerata* and *Cotesia rubecula*. The hosts are the larvae of the large and small white cabbage butterflies, *Pieris brassicae* and *Pieris rapae*, respectively. *C. rubecula* is a specialist of *P. rapae* while *C. glomerata* is a generalist and parasitises both hosts. Thus, there is a coupling of the four interacting species. This particular system is of considerable interest as all four species have a wide global range and both hosts are common crop pests of *brassica* species, including commercial crops such as cabbage, cauliflower and kale. Both parasitoids in the system have been used as successful biological control agents against the hosts [4,21]. More generally our system serves as an analogue for other multi-species host-parasitoid systems. A key aspect of the system is that, when searching for hosts, the parasitoids are observed to aggregate in response to chemical signalling cues emitted by the crops or plants (e.g. *brassica* species) that the hosts are feeding upon. This phenomenon is widely reported for host-parasitoid systems, and laboratory studies using the *Pieris*–*Cotesia* system have been the subject of a number of publications. Research has shown that both parasitoid species respond differentially to volatile infochemicals from plants infested with high and low host densities. Regions of high infochemical concentration correspond to regions of high host number and responsiveness to odours from host infested leaves was shown to increase with an increase in the total number of feeding hosts. Further studies have considered plant-mediated indirect effects on the persistence of host-parasitoid communities and the ability of parasitoids to discriminate between infochemicals from a range of different plant-host complexes [8,9,35,36] (and references therein). In short, infochemicals play a key role in multi-trophic relationships.

Chemotaxis is defined as biased or directed migration in response to diffusible chemical cues, the motion being directed to regions of highest chemical concentration. The aggregative behaviour of the parasitoids in our system towards plant infochemicals emitted during host feeding can thus be described as a chemotactic response and the plant infochemicals can thus be considered as chemoattractants. Chemical analysis has revealed only minor differences between the volatile blends of *P. brassicae* and *P. rapae* infested *brassica* plants [35]. Hence, throughout this work, we consider a single chemoattractant which is produced in proportion to the total host density.

In this paper we model the interactions of the species within a continuous-time framework because of observed overlap in population interactions. Hence, the temporal dynamics of our host-parasitoid system are modelled by a coupled system of four ordinary differential equations. The multi-species interactions considered in our model exhibit oscillatory temporal dynamics and such population dynamics have long been a topic of interest in the literature [11,13,25]. When spatial interactions are also taken into consideration, by way of random motility of the four species and the chemoattractant and the

chemotactic response of the parasitoids to the chemoattractant, a system of five reaction-diffusion-chemotaxis equations is obtained. The system of equations models the spatio-temporal dynamics of our four species host-parasitoid community and the chemoattractant. In this paper we consider the interactions of the two hosts and two parasitoids in a one-dimensional domain.

A significant body of work has considered a variety of reaction-diffusion-chemotaxis models since the seminal work of Keller and Segel [14–16]. Reaction-diffusion-chemotaxis equations have been used to model a number of ecological and biomedical problems including aggregative behaviour of the slime mould *Dictyostelium discoideum* and bacterial colonies including *Escherichia coli* and *Salmonella* [12, 14–18, 34], and cell aggregation, especially in wound healing and cancer tumor growth [1, 2, 5–7, 19, 30] (see [20] for a summary of the literature). There have been, however, relatively few attempts to incorporate parasitoid chemotactic behaviour in models of multi-species host-parasitoid systems. The work of Schofield et al. [27, 28] however considers an individual-based stochastic model of chemically mediated parasitoid foraging in a two-species host-parasitoid system and we extend the reaction-diffusion-chemotaxis model that serves as a basis for their individual-based model. The model system we consider is also an extension of a reaction-diffusion model of our multi-species system discussed in an earlier work [21]. Specifically in this paper we consider the impact on the dynamics of the system of increasing the parasitoid chemotactic response. In effect we compare the impact of random and non-random (chemotactic) parasitoid searching behaviour on the dynamics of our multi-species system. We primarily contribute to *Pieris–Cotesia* research by highlighting qualitative population dynamics which are extremely difficult to determine experimentally. Furthermore, we uncover dynamical behaviour that has not been previously shown for our system (see [21]). Parasitoid chemotactic searching is shown to have a significant impact on the dynamics of our multi-species system.

In the subsequent sections the model system and parameters are introduced and stability analysis and bifurcation analysis of the homogeneous system and linear stability analysis of the chemotaxis system are carried out. The results of numerical simulations are then presented and finally discussed with reference to their mathematical and ecological implications.

## 2 The mathematical model

The mathematical model is based on a system of partial differential equations. Reaction kinetics modelling the interactions of the hosts and parasitoids are coupled with spatial motility and chemotaxis terms giving rise to a system of reaction-diffusion-chemotaxis equations. Spatial motility, the chemotactic response and population interactions occur continuously. The underlying temporal dynamics are represented by a system of ordinary differential equations. Both host species (in the absence of parasitism) are modelled as having logistic, density-dependent growth, with intrinsic growth rates  $r_1$  and  $r_2$  and carrying capacities  $K_1$  and  $K_2$ , respectively. Parasitism by both parasitoids is modelled by

an Ivlev functional response—a negative exponential function which accounts for a saturating maximum parasitism rate. *C. glomerata* parasitises *P. brassicae* at rate  $\alpha_1$  and *P. rapae* at rate  $\alpha_2$ . *C. rubecula* parasitises *P. rapae* at rate  $\alpha_3$ . The Ivlev functional response is similar to the Holling Type II functional response and is a standard function for modelling parasitism or predation [26,31]. The efficiency of parasitoid discovery of hosts is denoted by  $a_1$ ,  $a_2$  and  $a_3$ , constants that determine host escape and the number of hosts parasitised. Each parasitised host gives rise to  $e_1$ ,  $e_2$  and  $e_3$  next-generation parasitoids. In effect  $e_1$ ,  $e_2$  and  $e_3$  are the parasitoid conversion efficiencies of hosts to parasitoids. The parasitoids are subject to intrinsic mortality rates  $d_1$  (*C. glomerata*) and  $d_2$  (*C. rubecula*). The addition of spatial motility terms model the parasitoids and hosts as moving randomly in a spatial domain. The motility coefficients  $D_1$ ,  $D_2$ ,  $D_3$  and  $D_4$  of the four species are constants and determine the rate at which each species disperses randomly throughout the domain. The chemoattractant  $k$  is produced proportionally to the total host density ( $N + M$ ) at the rate  $r_3$  and decays at the rate  $d_3$ . The motility coefficient of the chemoattractant,  $D_5$ , is a constant and determines the rate at which the chemoattractant diffuses through the domain. The chemotactic response of both species of parasitoid is modelled as a linear response and the strength of the response is determined by the chemotaxis coefficients  $\chi_1$  and  $\chi_2$ . The full model system is thus as follows:

$$\begin{aligned}
 \frac{\partial N}{\partial t} &= \overbrace{D_1 \nabla^2 N}^{\text{random motility}} + \overbrace{r_1 N \left(1 - \frac{N}{K_1}\right)}^{\text{logistic growth}} - \overbrace{\alpha_1 P (1 - e^{-a_1 N})}^{\text{mortality due to parasitism}} \quad , \\
 \frac{\partial M}{\partial t} &= D_2 \nabla^2 M + r_2 M \left(1 - \frac{M}{K_2}\right) - \alpha_2 P (1 - e^{-a_2 M}) - \alpha_3 Q (1 - e^{-a_3 M}), \\
 \frac{\partial P}{\partial t} &= D_3 \nabla^2 P - \chi_1 \nabla \cdot (P \nabla k) + e_1 \alpha_1 P (1 - e^{-a_1 N}), \\
 &\quad + e_2 \alpha_2 P (1 - e^{-a_2 M}) - d_1 P, \tag{1} \\
 \frac{\partial Q}{\partial t} &= \overbrace{D_4 \nabla^2 Q}^{\text{random motility}} - \overbrace{\chi_2 \nabla \cdot (Q \nabla k)}^{\text{parasitoid chemotactic response}} \quad , \\
 &\quad + \overbrace{e_3 \alpha_3 Q (1 - e^{-a_3 M})}^{\text{growth due to parasitism}} - \overbrace{d_2 Q}^{\text{mortality}} \quad , \\
 \frac{\partial k}{\partial t} &= D_5 \nabla^2 k + \underbrace{r_3 (N + M)}_{\text{production}} - d_3 k,
 \end{aligned}$$

where  $N$  and  $M$  represent the density of hosts *P. brassicae* and *P. rapae*, respectively,  $P$  and  $Q$  represent the density of parasitoids *C. glomerata* and *C. rubecula* and  $k$  represents the concentration of the chemoattractant produced during feeding by the hosts.  $N = N(x, t)$  denotes local population density (organisms per area) at time  $t$  and spatial coordinate  $x$  (and likewise for  $M, P$ , and  $Q$ ).  $k = k(x, t)$  denotes local chemoattractant concentration at time  $t$  and spatial

coordinate  $x$ . The system is posed on a given domain  $\Omega$  with smooth boundary  $\partial\Omega$ . We impose either zero-flux Neumann boundary conditions (which could correspond to an experimental greenhouse setting) or zero Dirichlet boundary conditions (which corresponds to a field setting with a hostile external environment) on  $\partial\Omega$  along with appropriate initial conditions to close the system. In one-dimension,  $\Omega = (0, L)$ .

Nondimensionalising gives critical insight into the relative magnitudes of the parameters required to produce biologically reasonable behaviour. Using the following non-dimensional variables;  $t' = r_1t$ ,  $x' = \frac{x}{L}$ ,  $N' = \frac{N}{K_1}$ ,  $M' = \frac{M}{K_2}$ ,  $P' = \frac{P}{K_1}$ ,  $Q' = \frac{Q}{K_2}$ ,  $k' = \frac{k}{k_0}$  and dropping primes gives the nondimensionalised system:

$$\begin{aligned} \frac{\partial N}{\partial t} &= D_N \nabla^2 N + N(1 - N) - s_1 P(1 - e^{-\rho_1 N}), \\ \frac{\partial M}{\partial t} &= D_M \nabla^2 M + \gamma_1 M(1 - M) - s_2 P(1 - e^{-\rho_2 M}) - s_3 Q(1 - e^{-\rho_3 M}), \\ \frac{\partial P}{\partial t} &= D_P \nabla^2 P - \chi_P \nabla \cdot (P \nabla k) + c_1 P(1 - e^{-\rho_1 N}) + c_2 P(1 - e^{-\rho_2 M}) - \eta_1 P, \quad (2) \\ \frac{\partial Q}{\partial t} &= D_Q \nabla^2 Q - \chi_Q \nabla \cdot (Q \nabla k) + c_3 Q(1 - e^{-\rho_3 M}) - \eta_2 Q, \\ \frac{\partial k}{\partial t} &= D_k \nabla^2 k + \gamma_2(N + \gamma_3 M) - \eta_3 k, \end{aligned}$$

where  $D_N = \frac{D_1}{r_1 L^2}$ ,  $D_M = \frac{D_2}{r_1 L^2}$ ,  $D_P = \frac{D_3}{r_1 L^2}$ ,  $D_Q = \frac{D_4}{r_1 L^2}$ ,  $D_k = \frac{D_5}{r_1 L^2}$ ,  $\chi_P = \frac{\chi_1 k_0}{r_1 L^2}$ ,  $\chi_Q = \frac{\chi_2 k_0}{r_1 L^2}$ ,  $\rho_1 = a_1 K_1$ ,  $\rho_2 = a_2 K_2$ ,  $\rho_3 = a_3 K_2$ ,  $\gamma_1 = \frac{r_1}{r_2}$ ,  $\gamma_2 = \frac{r_3 K_1}{r_1}$ ,  $\gamma_3 = \frac{K_2}{K_1}$ ,  $s_1 = \frac{\alpha_1}{r_1}$ ,  $s_2 = \frac{\alpha_2 K_1}{\alpha_1 K_2}$ ,  $s_3 = \frac{\alpha_3}{r_1}$ ,  $c_1 = \frac{e_1 \alpha_1}{r_1}$ ,  $c_2 = \frac{e_2 \alpha_2}{r_1}$ ,  $c_3 = \frac{e_3 \alpha_3}{r_1}$ ,  $\eta_1 = \frac{d_1}{r_1}$ ,  $\eta_2 = \frac{d_2}{r_1}$  and  $\eta_3 = \frac{d_3}{r_1}$ .

### 2.1 Parameter values

The parameter discussed below have been informed by considerable laboratory and field experience of the species involved. Some can be estimated with more precision than others and all are likely to show considerable plasticity in the field. The values used have therefore been chosen to give a representative qualitative picture of the dynamics of the system. Parasitoid dispersal ( $D_3, D_4$ ) has been documented of the order of  $10^{-3}$  to  $10^{-4} \text{ m}^2\text{s}^{-1}$  [3, 10] and is taken to be of the order of  $10^{-4} \text{ m}^2\text{s}^{-1}$  in our model. Host dispersal ( $D_1, D_2$ ) is considered to be small in comparison and is hence taken to be of the order of  $10^{-5} \text{ m}^2\text{s}^{-1}$ . The dispersal of the chemoattractant is taken to be of the order of  $10^{-3} \text{ m}^2\text{s}^{-1}$  [27, 28]. The baseline chemotactic response of both parasitoids ( $\chi_1, \chi_2$ ) is of the order of  $10^{-4} \text{ m}^2\text{s}^{-1}\text{mol}^{-1}$  [27, 28]. The generational increase in population size of the host populations *P. brassicae* and *P. rapae* has been observed to be around 45 and 35%, respectively. *P. brassicae* has a higher reproductive rate due

to laying a greater number of eggs. Host growth rates are thus taken as  $r_1 = 0.45$  and  $r_2 = 0.35$ . Host carrying capacities are taken to be  $K_1 = 250$  and  $K_2 = 250$ . Both parasitoids have similar parasitism efficiency rates on their primary host. *C. glomerata* however is considered less efficient at parasitising *P. rapae*, thus we take  $a_1 = 0.01$ ,  $a_2 = 0.001$  and  $a_3 = 0.01$ . Observed annual percentage parasitism rates of around 35% are reported in Cameron and Walker [4]. Also, as a secondary host, *P. rapae* is subject to less parasitism by *C. glomerata*, so we take parasitism rates  $\alpha_1 = 0.35$ ,  $\alpha_2 = 0.1$  and  $\alpha_3 = 0.35$ . *C. glomerata* has a higher conversion efficiency on its primary host, but significantly less on *P. rapae* so we take conversion efficiencies to be  $e_1 = 0.4$ ,  $e_2 = 0.02$ ,  $e_3 = 0.3$ . *C. glomerata* has been observed to suffer greater mortality, due to infections and other environmental factors than *C. rubecula*, thus we take  $d_1 = 0.08$  and  $d_2 = 0.06$ . The chemoattractant  $k$  is produced with intrinsic increase rate  $r_3 = 0.000018$  and decays at the rate  $d_3 = 0.0045$  [27,28]. Time is scaled with host intrinsic generational growth rate  $r_1 = 0.45$  (which has units  $t^{-1}$ ) and we consider domains of length of the order of 10 to  $10^2$  m, corresponding to the sizes of large laboratory-based experimental domains up to agricultural fields. Given the above parameter values the baseline non-dimensional parameter set is thus:  $D_N = D_M = 0.0000008$ ,  $D_P = D_Q = 0.0000075$ ,  $D_k = 0.0000125$ ,  $\chi_P = 0.00015$ ,  $\chi_Q = 0.00015$ ,  $\rho_1 = 2.5$ ,  $\rho_2 = 0.25$ ,  $\rho_3 = 2.5$ ,  $\gamma_1 = 0.8$ ,  $\gamma_2 = 0.01$ ,  $\gamma_3 = 1$ ,  $s_1 = 0.8$ ,  $s_2 = 0.2$ ,  $s_3 = 0.8$ ,  $c_1 = 0.3$ ,  $c_2 = 0.004$ ,  $c_3 = 0.2$ ,  $\eta_1 = 0.2$ ,  $\eta_2 = 0.1$  and  $\eta_3 = 0.01$ . The one dimensional domain ( $\Omega$ ) on which the system of equations is solved is a line of length one unit, with  $0 \leq x \leq 1$ . The system is solved with initial conditions  $N(0) = 0.75, \forall x \in \Omega$ ,  $M(0) = 0.75, \forall x \in \Omega$ ,  $P(0) = 0.075e^{-125x^2}$ ,  $Q(0) = 0.075e^{-125x^2}$  and  $k(0) = 0$  when the domain is set up with Neumann zero-flux boundary conditions. The system is solved with initial conditions  $N(0) = 0.75e^{-100(x-0.5)^2}$ ,  $M(0) = 0.75e^{-100(x-0.5)^2}$ ,  $P(0) = 0.075e^{-125(x-0.5)^2}$ ,  $Q(0) = 0.075e^{-125(x-0.5)^2}$  and  $k(0) = 0$  when the domain is set up with zero Dirichlet boundary conditions. In the discussion section we also briefly discuss the implementation of stable steady-state initial conditions and spatially heterogeneous initial conditions.

The system was solved numerically using two different numerical methods—the Fortran NAG routine DO3PCF and the Femlab finite element package. The Fortran NAG routine DO3PCF solves the system of PDEs using the method of lines to first obtain a system of ODEs and then uses a backward differentiation method to integrate the ODEs. For the finite element approach using Femlab, Lagrange quadratic elements were used as basis functions and the backward Euler time-stepping method was implemented to integrate the equations. The numerical results obtained using both the NAG routine and finite element method agree very closely.

### 3 Steady states and stability analysis

The spatially homogeneous fixed points of system (2) are found by solution of the following equations:

$$\begin{aligned}
 0 &= N^*(1 - N^*) - s_1 P^*(1 - e^{-\rho_1 N^*}) \\
 0 &= \gamma_1 M^*(1 - M^*) - s_2 P^*(1 - e^{-\rho_2 M^*}) - s_3 Q^*(1 - e^{-\rho_3 M^*}) \\
 0 &= c_1 P^*(1 - e^{-\rho_1 N^*}) + c_2 P^*(1 - e^{-\rho_2 M^*}) - \eta_1 P^* \\
 0 &= c_3 Q^*(1 - e^{-\rho_3 M^*}) - \eta_2 Q^* \\
 0 &= \gamma_2(N^* + \gamma_3 M^*) - \eta_3 k^*
 \end{aligned}$$

There are a number of biologically relevant, non-negative, equilibrium states including the unstable trivial state  $(0, 0, 0, 0, 0)$ , the unstable host only state  $(1, 1, 0, 0, k^*)$  and the unstable states  $(N^*, M^*, P^*, 0, k^*)$  and  $(N^*, M^*, 0, Q^*, k^*)$  where only one parasitoid is present in the system. We are however primarily interested in the stability of the unique coexistent state  $(N^*, M^*, P^*, Q^*, k^*)$ . For the baseline parameter set (see Subsect. 2.1), the unique coexistent equilibrium is:

$$N^* = 0.3379, \quad M^* = 0.3389, \quad P^* = 0.5043, \quad Q^* = 0.3716, \quad k^* = 0.6768$$

Linear stability analysis confirms that this equilibrium is stable (for the baseline parameter set). However it is of interest to determine whether any bifurcations occur when some of the key parameters are varied. In particular, previous work [21] has shown that the parameters  $\rho_i$  are important. Indeed a bifurcation analysis of the spatially homogeneous system, carried out using the XPP Auto package and varying the  $\rho_i$ , highlights the presence of a Hopf-bifurcation, which gives rise to temporal oscillations. The Hopf-bifurcation occurring when  $\rho_1 = 3.168$  and  $\rho_3 = 3.276$  is of considerable interest and has been shown in a previous work to have a significant impact on the spatio-temporal dynamics of the system in the absence of chemotaxis. We discuss this impact in the following section (see also [21]).

Linear analysis can be carried out to determine the (linear) stability of the unique coexistent steady state to small spatio-temporal perturbations. Linearising about the steady state in the usual way by setting:  $N = N^* + \epsilon \bar{N}(\mathbf{x}, t)$ ,  $M = M^* + \epsilon \bar{M}(\mathbf{x}, t)$ ,  $P = P^* + \epsilon \bar{P}(\mathbf{x}, t)$ ,  $Q = Q^* + \epsilon \bar{Q}(\mathbf{x}, t)$ ,  $k = k^* + \epsilon \bar{k}(\mathbf{x}, t)$ , we arrive at the following equation:

$$\underline{\omega}_t = \mathbf{A} + \mathbf{D} \nabla^2 \underline{\omega}$$

where  $\underline{\omega} = (\bar{N}, \bar{M}, \bar{P}, \bar{Q}, \bar{k})^T$ ,  $\mathbf{A}$  is the Jacobian matrix of the spatially homogeneous system and  $\mathbf{D}$  is a matrix of the diffusion and chemotaxis coefficients:

$$\mathbf{D} = \begin{bmatrix} D_N & 0 & 0 & 0 & 0 \\ 0 & D_M & 0 & 0 & 0 \\ 0 & 0 & D_P & 0 & -\chi_P P^* \\ 0 & 0 & 0 & D_Q & -\chi_Q Q^* \\ 0 & 0 & 0 & 0 & D_k \end{bmatrix}.$$

Assuming that solutions of the linearised system are proportional to:  $\omega = e^{\lambda t + i\kappa x}$  and following the standard linear stability analysis (see, for example, [18,20]) leads to the following system:

$$\lambda \underline{\omega} = \mathbf{A} \underline{\omega} - \mathbf{D} \kappa^2 \underline{\omega}$$

where  $\kappa$  is the spatial wave number.

The eigenvalues ( $\lambda$ ) are found from solution of the following characteristic polynomial:

$$|(\mathbf{A} - \mathbf{D} \kappa^2) - \lambda \mathbf{I}| = 0$$

which is a fifth order polynomial in terms of  $\lambda$  and  $\kappa$ . Solving the characteristic polynomial allows dispersion curves to be plotted which show how the value of the real part of the eigenvalues ( $\Re(\lambda)$ ) varies with  $\kappa$ . When the chemotaxis coefficients ( $\chi_P, \chi_Q$ ) are set to zero, for all  $\kappa$ , the largest  $\Re(\lambda) < 0$ , the required condition for equilibrium stability. Therefore the system is not subject to diffusion-driven instability. Thus, if the chemotaxis coefficients are non-zero, any change in the stability properties of the spatial system, must be “taxi driven”. That is, if for any values of  $\kappa$ , the largest  $\Re(\lambda) > 0$ , this is due to the effect of chemotaxis.

Figure 1 shows the dispersion curves for  $\chi_P = \chi_Q = 0$  (top left),  $\chi_P = \chi_Q = 0.000535$  (top right),  $\chi_P = \chi_Q = 0.000545$  (bottom left) and  $\chi_P = \chi_Q = 0.0015$  (bottom right). The top left dispersion curve highlights that for zero chemotaxis the system is stable, i.e. for all  $\kappa$ ,  $\Re(\lambda) < 0$ . Thus it is not possible to destabilise the system if  $\chi_P = \chi_Q = 0$ . The plot for  $\chi_P = \chi_Q = 0.000535$  shows that for all  $\kappa$ ,  $\Re(\lambda) < 0$ , confirming that small non-zero chemotaxis strength will not destabilise the system. The plot for  $\chi_P = \chi_Q = 0.000545$  however highlights that, for a range of values of  $\kappa$ ,  $\Re(\lambda) < 0$ . Thus, for  $\chi_P = \chi_Q = 0.000545$ , the system is unstable. There is clearly a threshold chemotaxis strength above which the system is destabilised. As the chemotaxis strength is increased the system is destabilised for a greater range of  $\kappa$ . For a larger range of values of  $\kappa$ ,  $\Re(\lambda) > 0$ , with the peak value of  $\Re(\lambda) \gg 0$ . The impact on the spatio-temporal dynamics of the behaviour uncovered by the linear analysis is highlighted in the following section.

#### 4 Spatio-temporal dynamics

The spatio-temporal dynamics of our system in the absence of chemotaxis have been considered in depth in a previous work [21]. The Hopf-bifurcation occurring when  $\rho_1 = 3.168$  and  $\rho_3 = 3.276$  is of considerable interest and has a significant impact on the spatio-temporal dynamics of the system in the absence of chemotaxis. For the baseline parameter set, with  $\rho_1 = \rho_3 = 2.5$ , the underlying spatially homogeneous steady-state is stable. As expected standard travelling waves of constant shape are observed as the parasitoids invade the host-only

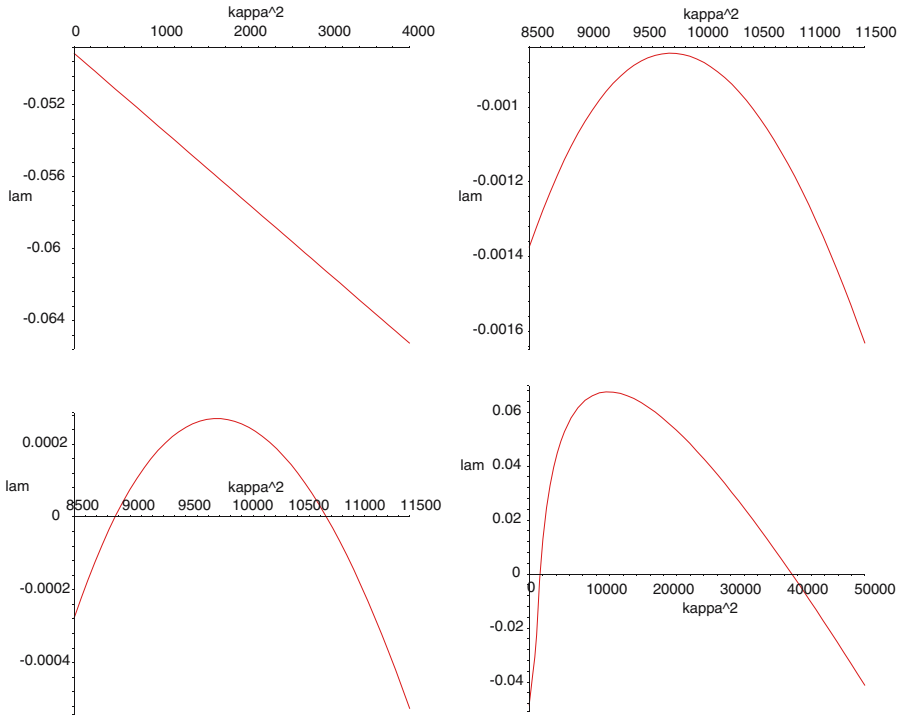


**Fig. 1** Dispersion curves of  $\kappa^2$  ( $x$ -axis) against the largest  $\mathbb{R}(\lambda)$  ( $y$ -axis) for  $\chi_P = \chi_Q = 0$  (top left),  $\chi_P = \chi_Q = 0.000535$  (top right),  $\chi_P = \chi_Q = 0.000545$  (bottom left) and  $\chi_P = \chi_Q = 0.0015$  (bottom right). As chemotaxis strength is increased the system becomes increasingly unstable ( $\mathbb{R}(\lambda) > 0$  for a larger range of values of  $\kappa$ )

domain. In the wake of the invasion fronts all four populations are at steady state and the system converges to the four-species steady state following invasion of the parasitoids through the domain. In the unstable region beyond the Hopf-bifurcation, with  $\rho_1 = \rho_3 = 4$ , the dynamics are dramatically different. Quasi-chaotic travelling waves give rise to domain wide heterogeneous patterns following parasitoid invasion of the domain.

The results of the linear stability analysis suggest that when the strength of the parasitoid chemotactic response is increased beyond a threshold level, the underlying steady-state will be destabilised, which in turn will affect the spatio-temporal dynamics. Thus we are primarily interested in the impact of increasing chemotaxis strength on the spatio-temporal dynamics of the system. We consider the cases where the coexistent steady-state is (1) stable and (2) unstable (i.e. a limit cycle is present), in the absence of chemotaxis.

When the baseline chemotactic response of  $\chi_P = \chi_Q = 0.00015$  is considered no significant qualitative change in the spatio-temporal dynamics in either the stable or unstable (limit-cycle) case is observed. Standard travelling waves of parasitoid invasion are observed when the underlying spatially homogeneous steady-state is stable (see Fig. 2) while quasi-chaotic waves are observed to give

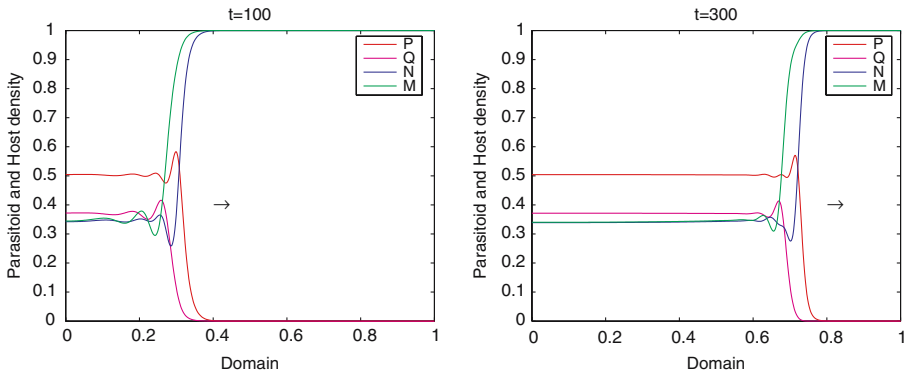


**Fig. 2** Snapshots of the 1-D dynamics of  $N, M, P, Q$  at the generation times  $t = 100, 300$  when  $\chi_P = \chi_Q = 0.00015$ . In the two sub-figures, host  $N$  is represented by a blue line, host  $M$  a green line, parasitoid  $P$  a red line and parasitoid  $Q$  a pink line. The four species interact in the domain  $\Omega = (0, 1)$  with zero flux boundary conditions set up on  $\partial\Omega$ . For the initial conditions and parameter values discussed in the text, stable travelling waves of parasitoid invasion are observed when  $\rho_1 = \rho_3 = 2.5$  and  $\rho_2 = 0.25$  (spatially homogeneous system stable)

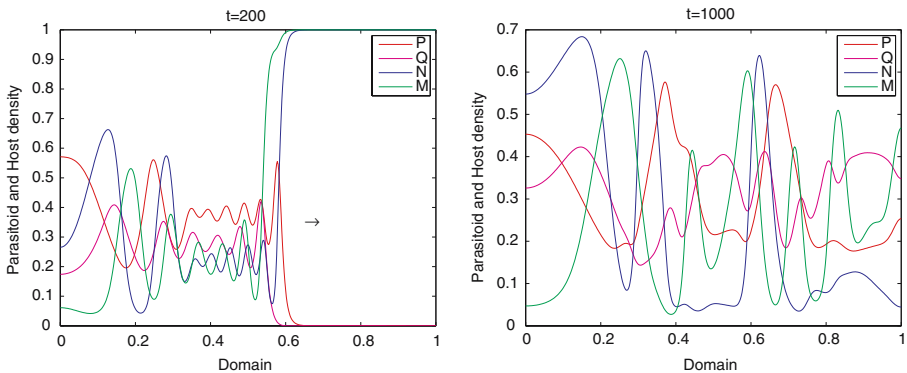


**Fig. 3** Snapshots of the 1-D dynamics of  $N, M, P$  and  $Q$  at the generation times  $t = 200, 1000$  when  $\chi_P = \chi_Q = 0.00015$ . In the two sub-figures, host  $N$  is represented by a blue line, host  $M$  a green line, parasitoid  $P$  a red line and parasitoid  $Q$  a pink line. The four species interact in the domain  $\Omega = (0, 1)$  with zero flux boundary conditions set up on  $\partial\Omega$ . For the initial conditions and parameter values discussed in the text, disordered, quasi-periodic wave behaviour is observed in the wake of the parasitoid invasion fronts when  $\rho_1 = \rho_3 = 4$  and  $\rho_2 = 0.4$  (spatially homogeneous system unstable). Persistent heterogeneous spatio-temporal dynamics are observed when the parasitoids have spread throughout the domain ( $t = 1000$ )

rise to domain wide multi-species heterogeneity when the spatially homogeneous steady-state is unstable (see Fig. 3). The observed dynamics correspond with the results of our linear stability analysis, which predict a threshold level of chemotaxis above which the system is subject to a taxis-driven instability. The baseline chemotaxis coefficients are below the destabilising threshold value so there is no change observed in the spatio-temporal dynamics of the system.

We now consider the case when the chemotactic response is just above the destabilising threshold ( $\chi_P = \chi_Q = 0.000545$ , see Fig. 1) and the underlying

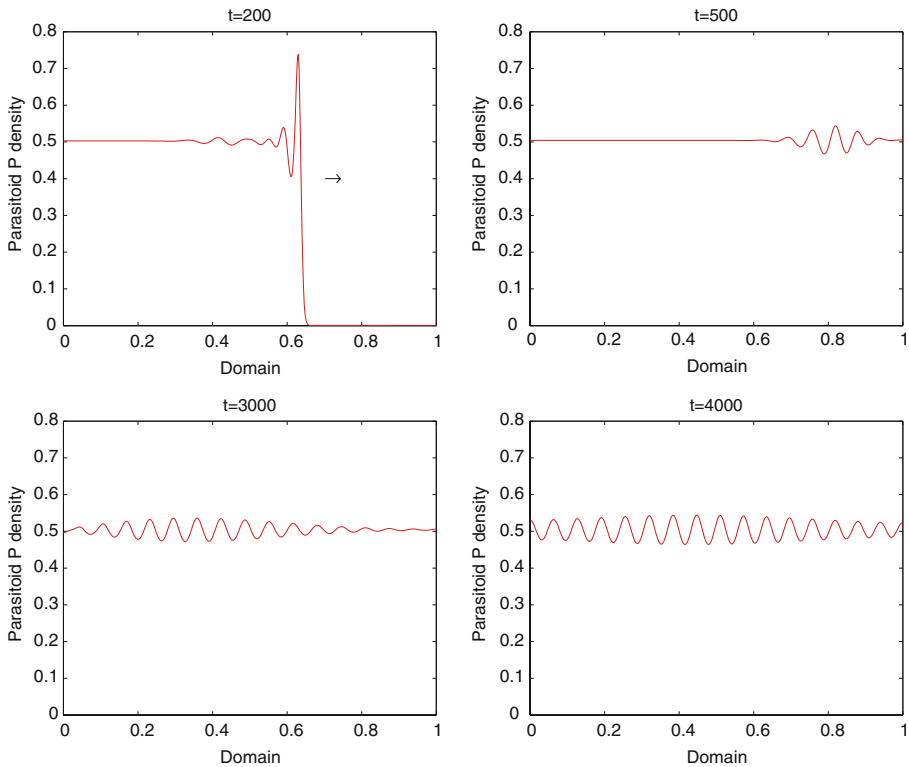


**Fig. 4** Snapshots of the 1-D dynamics of parasitoid  $P$  (represented by a red line) at the generation times  $t = 200, 500, 3000, 4000$  when  $\chi_P = \chi_Q = 0.000545$  and  $\rho_1 = \rho_3 = 2.5$  (spatially homogeneous system stable). The parasitoid  $P$  interacts with the other three species in the domain  $\Omega = (0, 1)$  with zero flux boundary conditions set up on  $\partial\Omega$ . For the initial conditions and parameter values discussed in the text, parasitoid chemotaxis response to the hosts gives rise to a domain-wide, stable heterogeneous spatio-temporal pattern

spatially homogeneous steady-state is stable. In this case the linear stability analysis carried out in the previous section predicts that chemotaxis will destabilise the coexistent steady-state. We may therefore expect that the solutions will evolve to a spatially heterogeneous steady-state. Figure 4 shows the results of a numerical simulation for  $\chi_P = \chi_Q = 0.000545$  and  $\rho_1 = \rho_3 = 2.5$ . For consistency we use the same initial conditions as before (although we note that the initial dynamics we observe can no longer be classified as travelling waves due to the destabilisation of the coexistent stable steady-state). Once the initial transient has spread through the domain, regular, small amplitude oscillations appear, initially in the left-half of the domain, before spreading throughout the entire domain (see Fig. 4). Qualitatively similar dynamics are observed for the other three species  $N, M, Q$  and the chemoattractant  $k$  (figures not shown). We expect to observe behaviour of this nature near the taxis destabilising threshold [16, 20]. The parasitoid chemotactic response to hosts has given rise to a spatially heterogeneous steady-state.

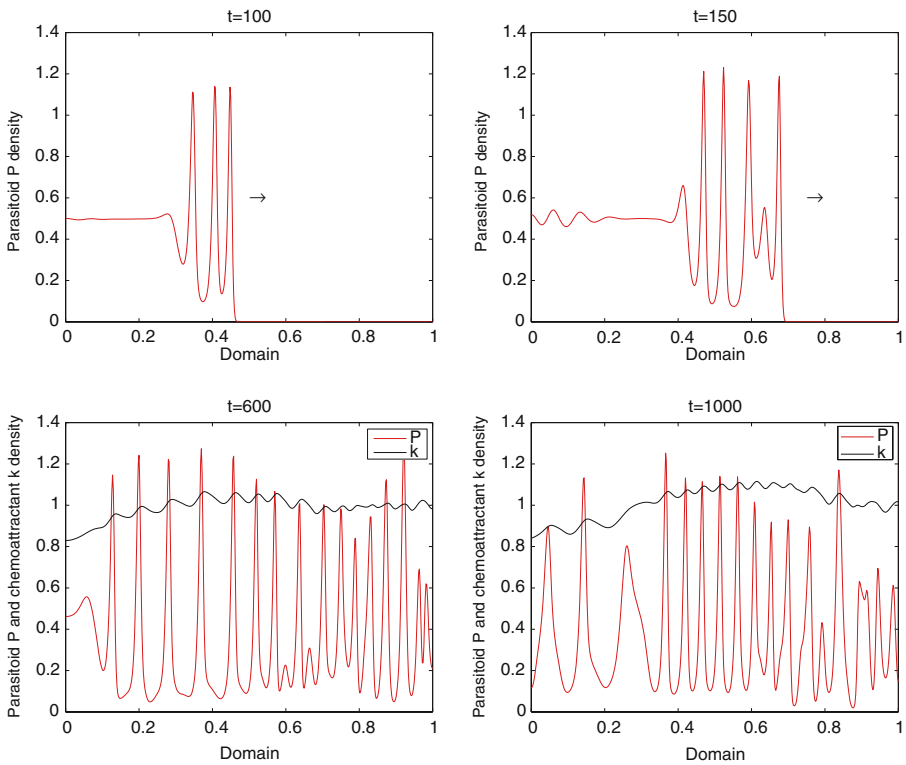


**Fig. 5** Snapshots of the 1-D dynamics of parasitoid  $P$  (represented by a red line) and the chemoattractant  $k$  (represented by a black line) at the generation times  $t = 100, 150, 600, 1000$  when  $\chi_P = \chi_Q = 0.0015$  and  $\rho_1 = \rho_3 = 2.5$  (spatially homogeneous system stable). The parasitoid  $P$  interacts with the other three species in the domain  $\Omega = (0, 1)$  with zero flux boundary conditions set up on  $\partial\Omega$ . For the initial conditions and parameter values discussed in the text, domain-wide, heterogeneous patterns are observed ( $t = 600, 1000$ ). Although quasi-ordered these patterns are not fixed and peaks are shown to both appear and be destroyed. A quasi-uniform chemoattractant concentration pattern, with small amplitude oscillations, is also observed ( $t = 600, 1000$ )

On a bounded domain,  $(0, 1)$ , the destabilising effect of chemotaxis (just above threshold) gives rise to a spatially heterogeneous steady-state pattern of mode number  $n$ , where  $n = \frac{\kappa}{\pi}$  and  $\kappa$  is the spatial wavenumber (see, [20]). Our numerical results correspond closely to the results predicted by the linear stability analysis. For the case presented in Fig. 4, the maximum value of  $\kappa$  is  $\kappa^2 \approx 9750$  (see the dispersion curve in Fig. 1 for  $\chi_P = \chi_Q = 0.000545$ ) and so  $n \approx 31$ , as observed in Fig. 4.

Given the impact of the parasitoid chemotactic response just above the destabilising threshold we are interested in the effect of further increasing the strength of the response (when the underlying dynamics are stable). Figure 5 shows the impact on the spatio-temporal dynamics when the chemotactic response is significantly increased (we consider  $\chi_P = \chi_Q = 0.0015$ ). Following the initial transient, large amplitude patterns of parasitoid  $P$  abundance are

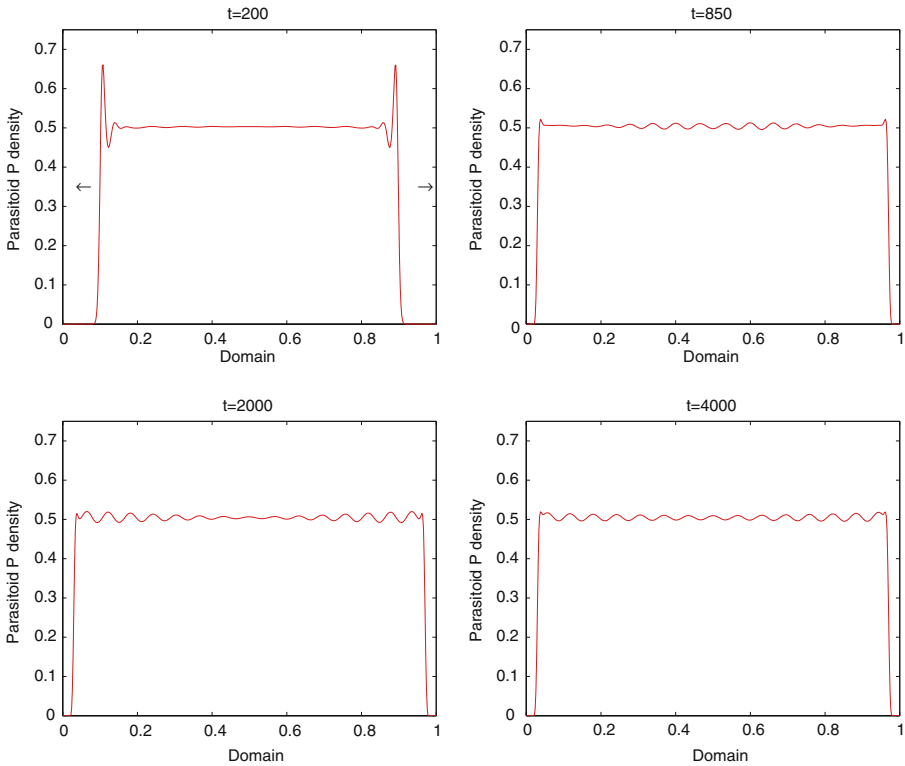


**Fig. 6** Snapshots of the 1-D dynamics of parasitoid  $P$  (represented by a red line) and the chemoattractant  $k$  (represented by a black line) at the generation times  $t = 200, 850, 2000, 4000$  when  $\chi_P = \chi_Q = 0.000545$  and  $\rho_1 = \rho_3 = 2.5$  (spatially homogeneous steady-state stable). The parasitoid  $P$  interacts with the other three species in the domain  $\Omega = (0, 1)$  with Dirichlet boundary conditions set up on  $\partial\Omega$ . The observed dynamics are qualitatively analogous to those when the domain is set up with zero-flux boundary conditions

shown to arise. Although there is some order to the patterns, their shape and position varies over time and we note that there is no fixed pattern, as was the case for chemotaxis just above threshold (see Fig. 4). The results of our linear stability analysis highlight that more than one spatial mode may be excited and the results of our simulation indicate this. Multiple spatial modes appear to have been excited and are interacting, with no single mode dominating, resulting in a spatio temporal pattern that is not fixed, with new peaks observed to appear over time. This result is similar to previous results discussed in [7] for models of cancer invasion. In Fig. 5 the corresponding profile for the chemoattractant is also plotted. The chemoattractant oscillates with small amplitude throughout the domain, with the peaks of chemoattractant corresponding to the peaks of parasitoid abundance, as expected from the form of the source term for  $k$ .

Having thus far used Neumann zero-flux boundary conditions, we now also briefly discuss the implementation of zero Dirichlet boundary conditions. As noted in Sect. 2, zero-flux boundary conditions correspond to an experimental

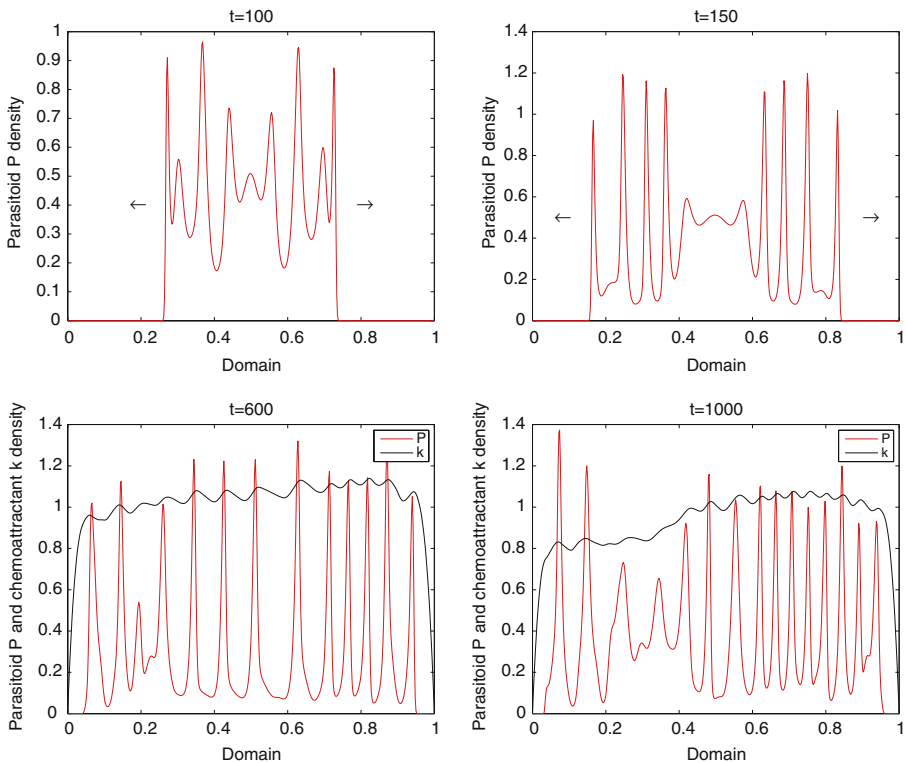


**Fig. 7** Snapshots of the 1-D dynamics of parasitoid  $P$  (represented by a red line) and the chemoattractant  $k$  (represented by a black line) at the generation times  $t = 100, 150, 600, 1000$  when  $\chi_P = \chi_Q = 0.0015$  and  $\rho_1 = \rho_3 = 2.5$  (spatially homogeneous steady-state stable). The parasitoid  $P$  interacts with the other three species in the domain  $\Omega = (0, 1)$  with Dirichlet boundary conditions set up on  $\partial\Omega$ . The observed dynamics are qualitatively analogous to those when the domain is set up with zero-flux boundary conditions

“greenhouse” environment where none of the species may escape from the domain, while zero Dirichlet boundary conditions correspond to a field setting with a hostile external environment. Figures 6 and 7 show the results of implementing zero Dirichlet boundary conditions on our domain. As is to be expected from the structure of the equations and a linear stability analysis, no significant qualitative change in the spatio-temporal dynamics is observed.

Increasing the parasitoid chemotactic response just above the destabilising threshold is observed to have a significant impact on the spatio-temporal dynamics of our system when the spatially homogeneous steady-state is unstable (limit-cycle). For chemotaxis below the threshold, disordered heterogeneous spatio-temporal patterns of parasitoid (and host) abundance are observed (see Fig. 3). However, considerably altered patterns are observed when  $\chi_P = \chi_Q = 0.000545$ . Ordered patterns, that are fixed in shape, arise following the initial transients of the parasitoids (see Fig. 8). The observed patterns represent peaks and troughs of parasitoid  $P$  abundance. Qualitatively

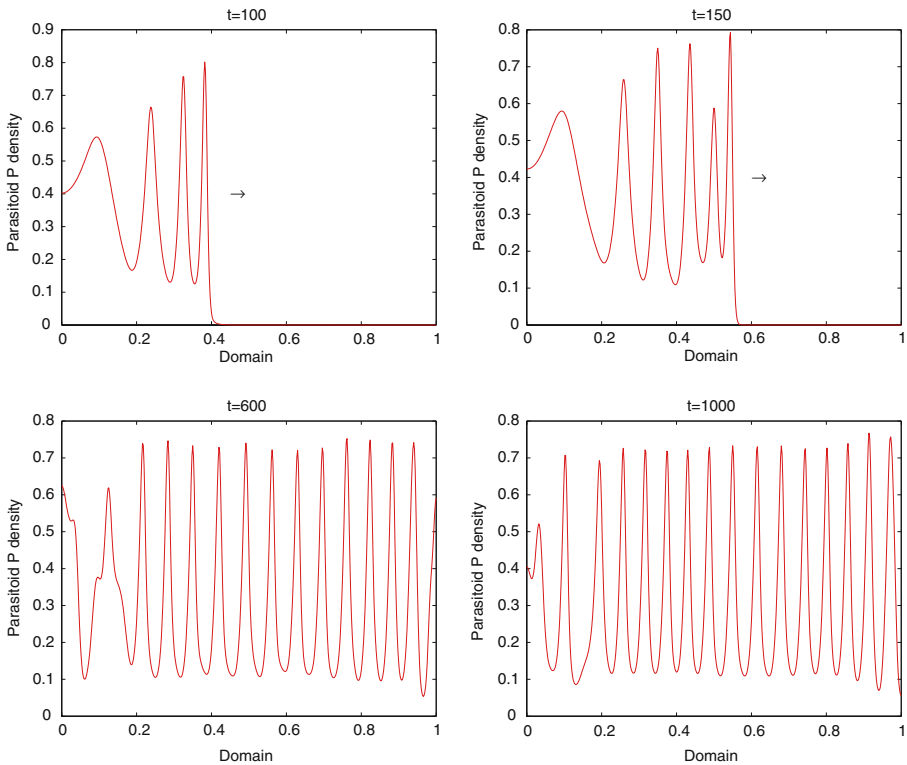


**Fig. 8** Snapshots of the 1-D dynamics of parasitoid  $P$  (represented by a red line) at the generation times  $t = 100, 150, 600, 1000$  when  $\chi_P = \chi_Q = 0.000545$  and  $\rho_1 = \rho_3 = 4$  (spatially homogeneous system unstable). The parasitoid  $P$  interacts with the other three species in the domain  $\Omega = (0, 1)$  with zero flux boundary conditions set up on  $\partial\Omega$ . For the initial conditions and parameter values discussed in the text the previously observed patterns of spatio-temporal heterogeneity have been replaced by fixed, stable heterogeneous patterns ( $t = 600, 1000$ )

similar patterns are observed for the other three species  $N, M, Q$  and the chemo-attractant  $k$  (figures not shown). Although no formal analysis can be carried out to determine the impact of chemotaxis on the system with underlying limit cycle dynamics, it is clear from our computational simulations that (in this case), chemotaxis also has a significant effect.

We have shown through linear stability analysis and computational simulations that parasitoid chemotactic response to regions of high host abundance has a significant (destabilising) impact on the spatio-temporal dynamics of the multi-species system whether the underlying spatially homogeneous steady-state is stable or unstable (limit-cycle). Comparing Figs. 4 and 8 highlights the somewhat qualitatively similar dynamical behaviour that arises under the destabilising influence of parasitoid chemotactic response just above threshold. However, the destabilising impact of chemotaxis brings about a more significant dynamical change when the underlying steady state is unstable (limit-cycle) with

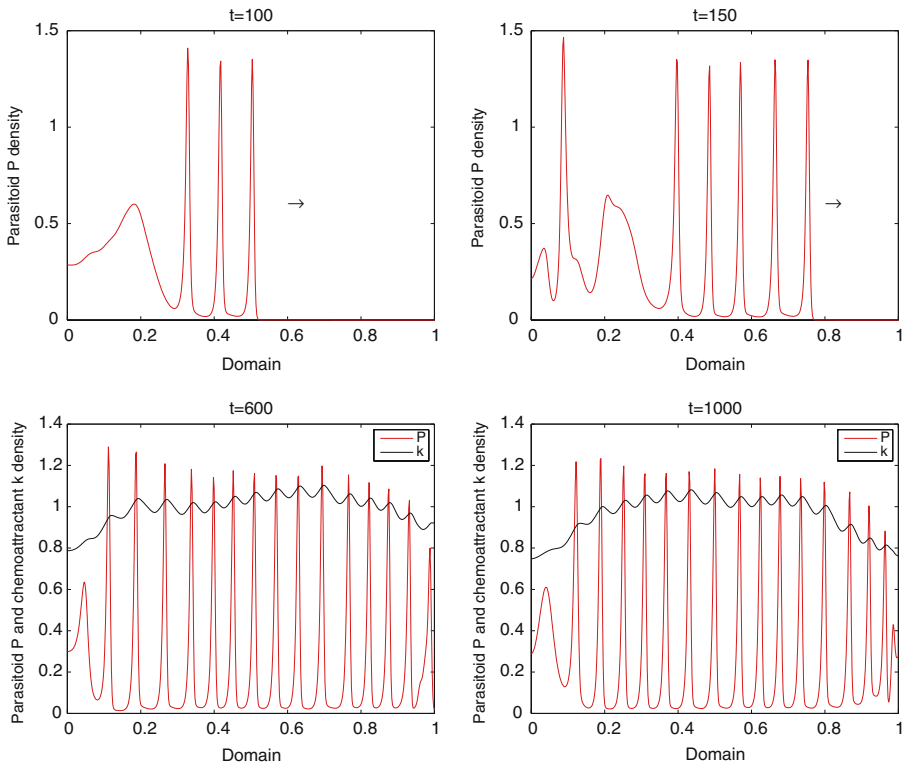


**Fig. 9** Snapshots of the 1-D dynamics of parasitoid  $P$  (represented by a red line) and the chemoattractant  $k$  (represented by a black line) at the generation times  $t = 100, 150, 600, 1000$  when  $\chi_P = \chi_Q = 0.0015$  and  $\rho_1 = \rho_3 = 4$  (spatially homogeneous system unstable). The parasitoid  $P$  interacts with the other three species in the domain  $\Omega = (0, 1)$  with zero flux boundary conditions set up on  $\partial\Omega$ . For the initial conditions and parameter values discussed in the text, ordered patterns of almost fixed shape are observed ( $t = 600, 1000$ ). The pattern is also shown to shift in space. An ordered chemoattractant concentration pattern with small amplitude oscillations is also observed ( $t = 600, 1000$ )

“order” being imposed on previously disordered quasi-chaotic heterogeneous dynamics.

Finally, when the underlying spatially homogeneous steady-state is unstable (limit-cycle), increasing the chemotaxis strength (again we consider  $\chi_P = \chi_Q = 0.0015$ ) a further dynamical change in the spatio-temporal patterns is observed. The results presented in Fig. 9 show that following the initial transients, ordered patterns of almost fixed shape arise. The patterns are qualitatively similar to those observed in Fig. 8 (and also somewhat qualitatively similar to those in Fig. 5). However, we observe that the position of these patterns varies, shifting in space over time. We have run our simulations for very long time periods (also with both boundary condition types) and Fig. 10 highlights that there is no convergence to a stable heterogeneous steady-state. We again note that this is consistent with the results of the linear stability analysis, highlighted in the

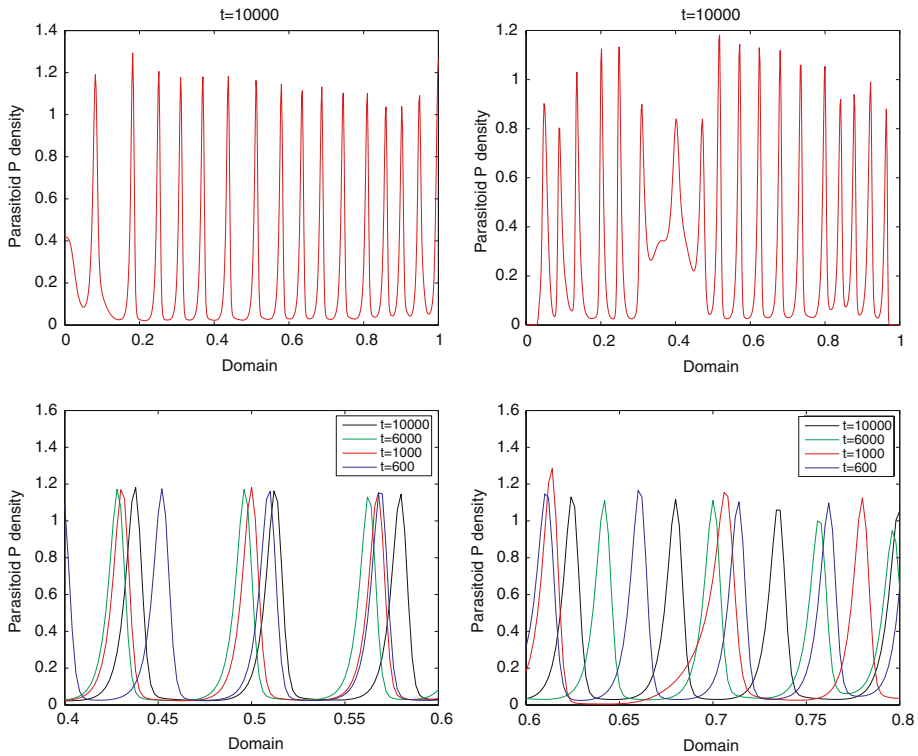


**Fig. 10** Snapshots of the 1-D dynamics of parasitoid  $P$  at the generation time  $t = 10000$  when  $\chi_P = \chi_Q = 0.0015$  and  $\rho_1 = \rho_3 = 4$  [spatially homogeneous steady-state unstable (limit-cycle)] with Neumann zero-flux (left hand sub figures) and zero Dirichlet (right hand sub figures) boundary conditions set up on  $\partial\Omega$ . Corresponding sub-figures show the dynamics of parasitoid  $P$  at generation times  $t = 600, 1000, 6000, 10000$  for sections of the domain. We highlight the temporal drift of the peaks

dispersion curve (for  $\chi_P = \chi_Q = 0.0015$ ) in Fig. 1. The dispersion curve shows that, for these values of chemotaxis, more than one spatial mode is excited. As we noted earlier, there is no guarantee of a final single dominant spatial mode producing a heterogeneous steady state. The results for the long time simulation runs appear to verify this point, as the spatio-temporal patterns persist dynamically and are not fixed (see Fig. 10).

All of the cases considered here highlight the impact of chemotaxis on the spatio-temporal dynamics of a multi-species host-parasitoid system, where the parasitoids respond chemotactically to plant infochemicals released during host feeding. It is clear that, for our system, the destabilising influence of the parasitoid chemotactic response over-rides the underlying stability properties of the spatially homogeneous system (and the corresponding spatio-temporal behaviour in the absence of chemotaxis), whether stable or unstable (limit-cycle). The mathematical and ecological implications of these impacts are considered in the following section.

## 5 Discussion

In this paper we have presented a mathematical model for a multi-species host-parasitoid system in which the parasitoids search chemotactically for hosts, mediated by plant infochemicals released during host feeding. The results of our model show that chemotactic searching by the parasitoids (i.e. an aggregative response to infochemical concentration) has a significant impact on the spatio-temporal dynamics of our multi-species system. Our results highlight several dynamical outcomes depending on whether the spatially homogeneous steady-state of the system is stable or unstable (i.e. a limit-cycle is present). We have primarily contributed to *Pieris–Cotesia* research by drawing attention to potential qualitative population dynamics that are extremely difficult to determine experimentally.

Our first result is the destabilisation of the steady state when the chemotactic response is above a threshold level. We first observe the appearance of a heterogeneous steady-state pattern for chemotaxis just above threshold. We also consider the impact of further increasing chemotaxis when the underlying dynamics are stable. The spatio-temporal patterns are no longer fixed and we see more complex behaviour including the appearance of new peaks. The appearance of a heterogeneous steady-state (for chemotaxis just above threshold) was an expected result. A number of previous works have specifically considered the destabilising impact of chemotactic responses on the dynamics of a variety of biological systems including slime mould, bacterial colonies and interacting cells. The work of Keller and Segel [14–16] discusses chemotactic initiation of migrating bands and regards aggregation as an instability, while other works have considered chemotaxis-driven pattern formation [12, 19, 20, 34].

Limited work, however, has considered the impact of parasitoid chemotactic response on the dynamics of multi-species host-parasitoid communities. The work of Schofield et al. [27, 28] considers an individual-based model of a two species host-parasitoid system and the authors conclude that parasitoids adopting chemically mediated strategies give rise to a dynamically unstable patchy distribution of hosts and parasitoids [27]. However the authors also note that addition of chemotaxis to their continuum model makes little or no qualitative difference to the long-term population dynamics [28]. This is not the case for our continuum model of a multi-species community where the addition of chemotaxis makes a significant qualitative difference to the population dynamics.

The second result to emerge from the computational simulations of our model is the impact of chemotaxis on the dynamics of the system when the underlying spatially homogeneous steady state is unstable (i.e. a limit-cycle is present). In the absence of chemotaxis and under low levels of chemotaxis, underlying limit-cycle kinetics give rise to quasi-chaotic heterogeneous spatio-temporal patterns. However, when chemotactic strength is increased just beyond the destabilising threshold, the disordered heterogeneous patterns are replaced by steady-state heterogeneous patterns which are significantly different. As chemotaxis is increased, ordered patterns of almost fixed shape arise.

However, the patterns are not fixed in space and shift over time. The patterns bear some qualitative similarity to the dynamics when the underlying homogeneous steady-state is stable. It is clear that when the parasitoid chemotactic response is strong, the spatially homogeneous dynamics of the system have little bearing on the spatio-temporal dynamics. The destabilising influence of the parasitoid chemotactic response over-rides the other mechanisms that initiate dynamical behaviour. Although the results of our linear stability analysis predict a threshold chemotaxis strength above which the system will be destabilised and the possibility of fixed heterogeneous patterns, they give less indication of the dynamical behaviour that we observe when chemotaxis strength is increased.

There are several ecological implications of our results. Firstly, it is clear that if the chemotactic response of dispersing parasitoids to plant infochemicals is sufficiently strong (above a threshold level) there is no stable spatio-temporal outcome possible. In the absence of chemotaxis the multi-species system is stable for the baseline parameter set. However, we observe the appearance of a domain-wide heterogeneous steady-state when chemotaxis is just above a threshold level. Thus we have shown that if parasitoids respond chemotactically to hosts, multi-species host-parasitoid interactions may never achieve a stable spatio-temporal state, regardless of the underlying dynamics of the spatially homogeneous system. This outcome highlights the importance of considering spatio-temporal interactions.

A further ecological implication concerns the significance of increasing the parasitoid chemotactic response. The model results highlight that increasing the chemotactic response has a significant dynamical impact. In ecological terms, setting the chemotaxis coefficient to zero is analogous to modelling random parasitoid foraging behaviour. Parasitoids are modelled as dispersing randomly throughout a given domain. Random parasitoid searching has been shown to give rise to a wide range of spatio-temporal dynamics depending on the underlying spatially homogenous dynamics (see Sect. 4 and [21]). However, as discussed in the introduction, there is considerable evidence to suggest that parasitoids do not search randomly but aggregate in response to plant infochemicals released during host feeding [8,9,28,35,36]. Furthermore parasitoid searching behaviour has been shown to have a degree of plasticity and both *C. glomerata* and *C. rubecula* exhibit improved searching ability as a result of learned experience [8,9] (and references therein). Thus, increasing the chemotaxis coefficients can be viewed as equivalent to modelling an improved and more effective searching ability of parasitoids that can occur over a parasitoid's life span due to learned experience. The impact of increasing the chemotactic response on the spatio-temporal dynamics is significant and is shown to have the potential to over-ride all other spatio-temporal dynamics and the mechanisms that generate them.

We now show computational results we obtain from solving our system using different initial conditions (see Figs. 11, 12). If we set the chemotactic response to a value above the destabilising threshold and a small perturbation is applied to the spatially homogeneous steady-state, the stable steady-state is destabilised and the perturbation initiates a domain-wide heterogeneous steady-state. This result is expected from the linear stability analysis. In Fig. 11 we show the results

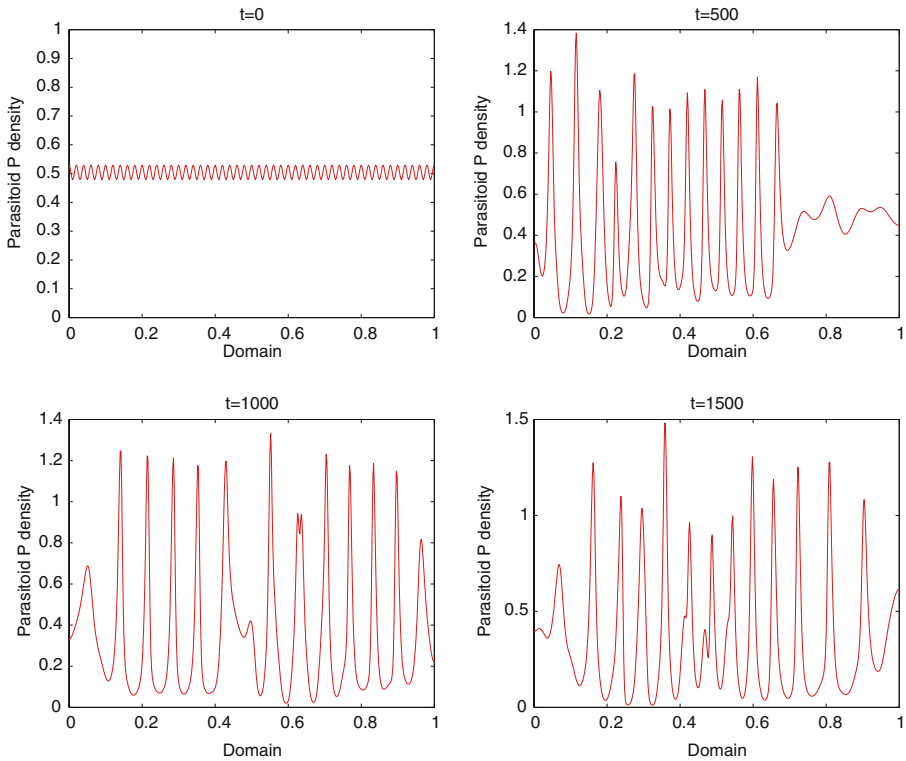


**Fig. 11** Snapshots of the 1-D dynamics of parasitoid  $P$  (represented by a red line) at the generation times  $t = 0, 500, 1000, 1500$  when  $\chi_P = \chi_Q = 0.0015$  and  $\rho_1 = \rho_3 = 2.5$  (spatially homogeneous system stable). The parasitoid  $P$  interacts with the other three species in the domain  $\Omega = (0, 1)$  with zero flux boundary conditions set up on  $\partial\Omega$ . For the initial conditions (stable steady state) and parameter values discussed in the text, domain-wide, heterogeneous patterns are observed ( $t = 500, 1000, 1500$ ). Although there is some order, these patterns are not fixed and new peaks are shown to appear. The patterns are analogous those shown in Fig. 5

of perturbing the stable homogeneous steady-state when  $\chi_P = \chi_Q = 0.0015$ . The dynamics we observe are analogous to those discussed in Sect. 4 (see also Fig. 5). When the system is solved using spatially heterogeneous initial conditions, the impact of increasing chemotaxis above threshold is also as previously discussed (see Fig. 12 and also Fig. 9). Figure 12 again shows the results for  $\chi_P = \chi_Q = 0.0015$ .

Implementing these alternative initial conditions also has ecological implications. Many environmental factors could result in our system being perturbed. Thus, whether the system is at its stable spatially homogeneous steady-state or in a heterogeneous dynamical state (limit-cycle kinetics), if the chemotactic response of the parasitoids changes over time and increases above a destabilising threshold (which could occur over time as a learned response, [29]) any perturbation will result in a potentially significant change in the dynamical state of the system. Thus the interplay of an environmental perturbation and

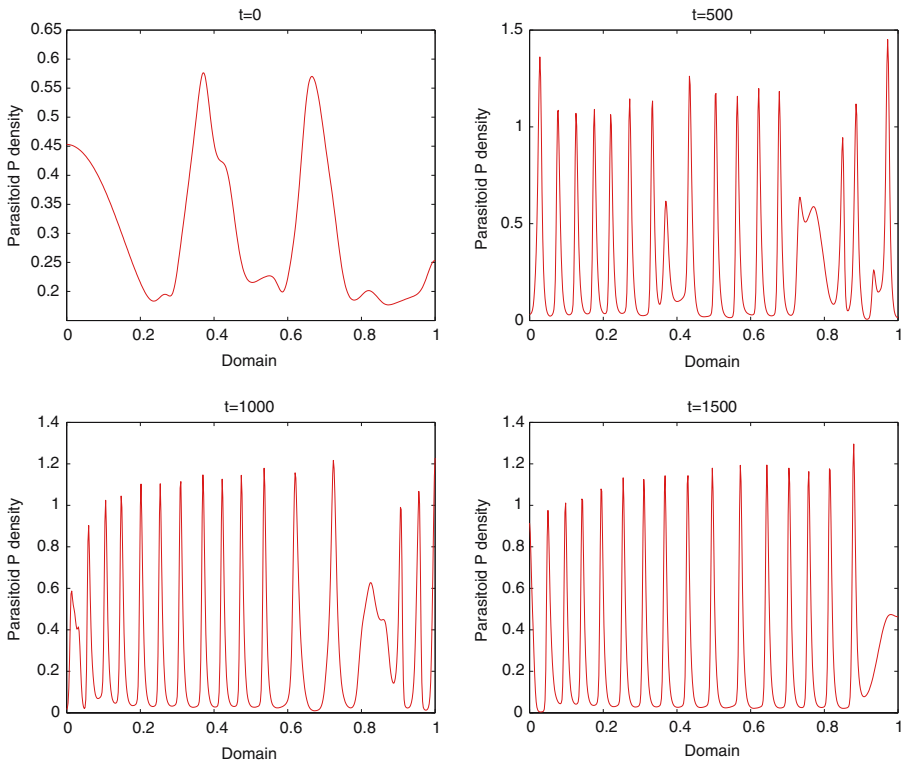


**Fig. 12** Snapshots of the 1-D dynamics of parasitoid  $P$  (represented by a red line) at the generation times  $t = 0, 500, 1000, 1500$  when  $\chi_P = \chi_Q = 0.0015$  and  $\rho_1 = \rho_3 = 4$  (spatially homogeneous system unstable). The parasitoid  $P$  interacts with the other three species in the domain  $\Omega = (0, 1)$  with zero flux boundary conditions set up on  $\partial\Omega$ . For the initial conditions (heterogeneous) and parameter values discussed in the text, ordered patterns of almost fixed shape, that shift in space, are observed ( $t = 500, 1000, 1500$ ). The patterns are analogous to those shown in Fig. 9

improved parasitoid searching ability could act to destabilise the spatio-temporal dynamics of a multi-species system.

We note that our work can also be viewed in the wider context of invasion and pattern formation in ecological systems modelled by reaction-diffusion equations. The seminal work of Sherratt et al. [31,32] demonstrated the existence of both regular and irregular (chaotic) spatiotemporal oscillations in the wake of invasive waves of predators in reaction-diffusion models of predator-prey interactions. The systems were studied on large spatial domains. The subsequent work of Malchow and Petrovskii [22,23] analysed a predator-prey system on a finite domain. They demonstrated the initiation of spatio-temporal chaos via a different mechanism—by perturbing the spatially homogeneous steady-state of a reaction-diffusion predator-prey system with underlying limit-cycle kinetics. For a wide class of initial conditions chaotic patterns are observed to first appear in a sub-domain before growing and invading the whole domain. The authors calculate the minimum speed of invasion and conclude that once a chaotic

pattern arises at a particular spatial location it will always invade the whole domain. The authors also observe spatially heterogeneous patterns which vary slowly and gradually in time (the local temporal behaviour of the predator and prey following the limit-cycle of the underlying ODE kinetics). We note that the potential role played by boundary conditions in determining spatio-temporal behaviour of oscillatory reaction-diffusion equations has also been a focus of recent interest [33]. A change of boundary conditions from zero-flux to zero Dirichlet has been shown to result in the initiation of heterogeneous spatio-temporal behaviour in reaction-diffusion systems with limit-cycle kinetics. Specific examples are given in [33]. Finally, chaotic dynamics have been observed in a recent model of a multi-species host-parasitoid system with disease dynamics [24]. In this system, the underlying ODE system itself is shown to have a chaotic attractor. When diffusion is included and the associated system of PDEs is solved numerically on a finite domain, dynamic heterogeneous spatio-temporal patterns are observed.

It is now widely thought that heterogeneous dynamics and pattern formation are inherent in ecological systems where species disperse and their trophic interactions give rise to limit-cycle kinetics. Several mechanisms have been identified as responsible for generating them [21–23, 31–33]. In this paper we have shown that chemotaxis has the potential to initiate a range of spatio-temporal behaviour in our system and in particular, that destabilising chemotaxis can bring “order” to quasi-chaotic heterogeneous patterns.

Future work will continue to focus on the current model system. Greater biological realism will be incorporated by including model terms that account for the release of a separate chemoattractant by each host. Furthermore, differences in the parasitoid chemotaxis coefficients will be considered to uncover the impact of differences in the strength of the two parasitoid’s chemotactic response. This will allow us to consider the scenario of a randomly searching parasitoid population competing with a non-randomly searching population.

**Acknowledgments** The authors thank an anonymous referee for helpful constructive comments of an earlier version of the paper.

## References

1. Alt, W., Lauffenburger, D.A.: Transient behaviour of a chemotaxis system modelling certain types of tissue inflammation. *J. Math. Biol.* **24**, 691–722 (1985)
2. Anderson, A.R.A., Chaplain, M.A.J.: Continuous and discrete mathematical models of tumor-induced angiogenesis. *Bull. Math. Biol.* **60**, 857–899 (1998)
3. Barlow, N.D., Beggs, J.R., Moller, H.: Spread of the wasp parasitoid *Sphecohyga vesparum* following its release in New Zealand. *N.Z. J. Ecol.* **22**(2), 205–208 (1998)
4. Cameron, P.J., Walker, G.P.: Field evaluation of *Cotesia rubecula*, an introduced parasitoid of *Pieris rapae* in New Zealand. *Biol. Control* **31**(2), 367–374 (2002)
5. Chaplain, M.A.J., Stuart, A.M.: A mathematical model for the diffusion of tumor angiogenesis factor into the surrounding host tissue. *IMA J. Math. Appl. Med. Biol.* **8**, 191–220 (1991)
6. Chaplain, M.A.J., Stuart, A.M.: A model mechanism for the chemotactic response of endothelial cells to tumor angiogenesis factor. *IMA J. Math. Appl. Med. Biol.* **10**, 149–168 (1993)

7. Chaplain, M.A.J., Lolas, G.: Mathematical modelling of cancer cell invasion of tissue: the role of the urokinase plasminogen activation system. *Math. Model. Methods. Appl. Sci.*, **15**, 1685–1734 (2005)
8. Geervliet, J.B.F., Ariens, S., Dicke, M., Vet, L.E.M.: Long-distance assessment of patch profitability through volatile infochemicals by the parasitoids *Cotesia glomerata* and *Cotesia rubecula*. *Biol. Control* **11**, 113–121 (1998)
9. Geervliet, J.B.F., Vreugdenhill, A.I., Dicke, M., Vet, L.E.M.: Learning to discriminate between infochemicals from different plant-host complexes by the parasitoids *Cotesia glomerata* and *Cotesia rubecula*. *Entomol. Exp. Appl.* **86**, 241–252 (1998)
10. Goldson, S.L., Proffitt, J.R., McNeill, M.R., Baird, D.B.: Linear patterns of dispersal and build up of the introduced parasitoid *Microctonus hyperode* (Hymenoptera: Braconidae) in Canterbury, New Zealand. *Bull. Entomol. Res.* **89**(4), 347–353 (1999)
11. Hassell, M.P., Wilson, H.B.: The dynamics of spatially distributed host-parasitoid systems. In: Tilman D., Kareiva, P. (eds.) *Spatial Ecology*. Princeton University Press, USA (1997)
12. Höfer, T., Sherratt, J.A., Maini, P.K.: Cellular pattern formation during *Dictyostelium* aggregation. *Phys. D* **85**, 425–444 (1995)
13. Holt, R.D., Hassell, M.P.: Environmental heterogeneity and the stability of host-parasitoid interactions. *J. Anim. Ecol.* **62**, 89–100 (1993)
14. Keller, E.F., Segel, L.A.: Initiation of slime mould aggregation viewed as an instability. *J. Theor. Biol.* **26**, 399–415 (1970)
15. Keller, E.F., Segel, L.A.: Model for Chemotaxis. *J. Theor. Biol.* **30**, 225–234 (1971a)
16. Keller, E.F., Segel, L.A.: Travelling bands of chemotactic bacteria: a theoretical analysis. *J. Theor. Biol.* **30**, 235–248 (1971b)
17. Lauffenburger, D.A., Aris, R., Kennedy, C.R.: Travelling bands of chemotactic bacteria in the context of population growth. *Bull. Math. Biol.* **46**, 19–40 (1984)
18. Maini, P.K., Myerscough, M.R., Winters, K.H., Murray, J.D.: Bifurcating spatially heterogeneous solutions in a chemotaxis model for biological pattern generation. *Bull. Math. Biol.* **53**(5), 701–719 (1991)
19. McDougall, S.R., Anderson, A.R.A., Chaplain, M.A.J., Sherratt, J.A.: Mathematical modelling of flow through vascular networks: implications for tumor-induced angiogenesis and chemotherapy strategies. *Bull. Math. Biol.* **64**, 673–702 (2002)
20. Murray, J.D.: *Mathematical Biology. I: An Introduction. II: Spatial models and Biomedical Applications*. Springer, New York (2002)
21. Pearce, I.G., Chaplain, M.A.J., Schofield, P.G., Anderson, A.R.A., Hubbard, S.F.: Modelling the spatio-temporal dynamics of multi-species host-parasitoid interactions: heterogeneous patterns and ecological implications. *J. Theor. Biol.* **241**, 876–886 (2006)
22. Petrovskii, S.V., Malchow, H.: A minimal model of pattern formation in a predator-prey system. *Math. Comp. Model.* **29**(8), 49–63 (1999)
23. Petrovskii, S.V., Malchow, H.: Wave of chaos: new mechanism of pattern formation in spatio-temporal population dynamics. *Theor. Popul. Biol.* **59**, 157–174 (2001)
24. Preedy, K., Schofield, P.G., Chaplain, M.A.J., Hubbard, S.F.: Disease induced dynamics in host-parasitoid systems: Chaos and coexistence. *R. Soc. Interface*, doi: 10.1098/rsif.2006.0184 (2006)
25. Rohani, P., Miramontes, O.: Chaos or quasiperiodicity in laboratory insect populations? *J. Anim. Ecol.* **65**(6), 847–849 (1996)
26. Savill, N.J., Rohani, P., Hogeweg, P.: Self-reinforcing spatial patterns enslave evolution in a host-parasitoid system. *J. Theor. Biol.* **188**, 11–20 (1997)
27. Schofield, P.G., Chaplain, M.A.J., Hubbard, S.F.: Mathematical modelling of host-parasitoid systems: effects of chemically mediated parasitoid foraging strategies on within- and between-generation spatio-temporal dynamics. *J. Theor. Biol.* **214**, 31–47 (2002)
28. Schofield, P.G., Chaplain, M.A.J., Hubbard, S.F.: Dynamic heterogeneous spatio-temporal pattern formation in host-parasitoid systems with synchronised generations. *J. Math. Biol.* **50**, 559–583 (2005)
29. Schofield, P.G., Chaplain, M.A.J., Hubbard, S.F.: Evolution of searching and life history characteristics in individual-based models of host/parasitoid/microbe associations. *J. Theor. Biol.* **237**, 1–16 (2005)
30. Sherratt, J.A.: Chemotaxis and chemokinesis in eukaryotic cells: the Keller–Segel equations as an approximation to a detailed model. *Bull. Math. Biol.* **56**, 129–146 (1994)

31. Sherratt, J.A., Lewis, M.A., Fowler, A.C.: Ecological chaos in the wake of invasion. *Proc. Natl. Acad. Sci. USA* **92**, 2524–2528 (1995)
32. Sherratt, J.A., Eagan, B.T., Lewis, M.A.: Oscillations and chaos behind predator-prey invasion: mathematical artifact or ecological reality? *Phil. Trans. R. Soc. Lond. B* **352**, 21–38 (1997)
33. Sherratt, J.A.: Periodic travelling wave selection by Dirichlet boundary conditions in oscillatory reaction-diffusion systems. *SIAM. J. Appl. Math.* **63**(5), 1520–1538 (2003)
34. Tyson, R.C., Lubkin, S.R., Murray, J.D.: Model and analysis of chemotactic patterns in a liquid medium. *J. Math. Biol.* **38**, 359–375 (1999)
35. Poecke, R.M.P. van , Roosjen, M., Pumarino, L., Dicke, M.: Attraction of the specialist parasitoid *Cotesia rubecula* to *Arabidopsis thaliana* infested by host or non-host herbivore species. *Entomol. Exp. Appl.* **107**, 229–236 (2003)
36. Vos, M., Berrocal, S.M., Karamaouna, F., Hemerik, L., Vet, L.E.M.: Plant-mediated indirect effects and the persistence of parasitoid-herbivore communities. *Ecol. Lett.* **4**, 38–45 (2001)